MIT-CTP 4399, NT-LBL-12-015, UCB-NPAT-12-013, WUB/12-18

Nucleon Structure from Lattice QCD Using a Nearly Physical Pion Mass

J. R. Green,[1] M. Engelhardt,[2] S. Krieg,[3] J. W. Negele,[1] A. V. Pochinsky,[1] and S. N. Syritsyn[4,*]

[1] *Massachusetts Institute of Technology, Cambridge, Massachusetts 02139, USA*
[2] *Physics Department, New Mexico State University, Las Cruces, New Mexico 88003, USA*
[3] *Bergische Universität Wuppertal, D-42119 Wuppertal, Germany and IAS, Jülich Supercomputing Centre, Forschungszentrum Jülich, D-52425 Jülich, Germany*
[4] *Lawrence Berkeley National Laboratory, Berkeley, California 94720, USA*

(Dated: September 11, 2012)

We report the first lattice QCD calculation using the almost physical pion mass $m_\pi = 149$ MeV that agrees with experiment for four fundamental isovector observables characterizing the gross structure of the nucleon: the Dirac and Pauli radii, the magnetic moment, and the quark momentum fraction. The key to this success is excluding the contributions of excited states. An analogous calculation of the nucleon axial charge governing beta decay fails to agree with experiment, and we discuss possible sources of error.

PACS numbers: 12.38.Gc, 13.60.Fz

INTRODUCTION

Lattice QCD is the only known rigorous framework for ab-initio calculation of the structure of protons and neutrons with controllable errors. It can provide quantitative answers to both fundamental questions such as the quark and gluon composition of the nucleon spin and phenomenological questions such as the sensitivity of modern detectors to physics beyond the Standard Model (BSM), to fundamental symmetry violations, and to hypothetical dark matter particles [1–3]. However, with current computer resources, its predictive power is limited by uncertainties arising from heavier than physical quark masses, finite lattice spacing and volume, incomplete removal of excited states, and omission of disconnected contractions. Therefore, until exhaustive lattice calculations remove these uncertainties, reproducing several well-known experimental observables is an important way to increase confidence in lattice QCD predictions.

Significant effort has been focused on lattice calculations of several isovector quantities[1] such as the Dirac and Pauli radii $(r^2_{1,2})^v$, the axial charge g_A, and the quark momentum fraction $\langle x\rangle_{u-d}$:

$$\langle p'|\bar q\gamma^\mu q|p\rangle = \bar u_{p'}\big[F_1^q(Q^2)\gamma^\mu + F_2^q(Q^2)\frac{i\sigma^{\mu\nu}q_\nu}{2M}\big]u_p,$$
$$F^q_{1,2}(Q^2) \underset{Q^2\to 0}{\approx} F^q_{1,2}(0)\big(1-\frac{1}{6}(r^2_{1,2})^q Q^2 + \mathcal{O}(Q^4)\big), \quad (1)$$

$$\langle p|\bar q\gamma_{\{\mu}\overleftrightarrow{D}_{\nu\}}q|p\rangle = \langle x\rangle_q\ \bar u_p\gamma_{\{\mu}p_{\nu\}}u_p, \quad (2)$$

$$\langle p|\bar q\gamma^\mu\gamma^5 q|p\rangle = g_A\ \bar u_p\gamma^\mu\gamma^5 u_p\,, \quad (3)$$

where $Q^2 = -q^2 = -(p'-p)^2$ and u_p, $u_{p'}$ are nucleon spinors. Although some success has been achieved [4–9], past results rely heavily on large extrapolations using Chiral Perturbation Theory (ChPT) yielding potentially uncontrollable corrections. This is particularly problematic for some observables, e.g., $(r^2_{1,2})^v$ and $\langle x\rangle_{u-d}$, for which ChPT predicts rapid change towards the chiral regime, making extrapolations very difficult. For example, in typical lattice calculations with pion masses $\gtrsim 250$ MeV, prior to extrapolation to $m_\pi^{\rm phys}\approx 135$ MeV, $(r_1^2)^v$ is underestimated by $\approx 50\%$ [6–8, 10], $\langle x\rangle_{u-d}$ overestimated by $30-60\%$ [5, 11, 12], and g_A underestimated by $\approx 10\%$ [4, 13, 14], compared with experiment. These glaring discrepancies and the dependence on large extrapolations clearly indicate the need for calculations near the physical pion mass. Moreover, it has recently been found that excited-state effects become worse with decreasing pion mass [15], and their careful analysis is required before even attempting extrapolations in the pion mass towards the physical point using ChPT.

In this paper, we report the first lattice QCD calculation of nucleon structure using pion masses as light as $m_\pi = 149$ MeV and thus very close to the physical value; therefore, our results rely much less on ChPT extrapolations than previous calculations. For each ensemble, we remove excited-state contaminations by varying the source-sink separation in the range $\approx 0.9\ldots1.4$ fm and apply the summation method [16] to extract the ground state matrix elements. We observe remarkable agreement with experiment of the isovector Dirac and Pauli radii, the anomalous magnetic moment, and the quark momentum fraction, all computed with the same methodology. However, as we will see later, the axial charge g_A is still underpredicted and requires further studies.

* ssyritsyn@lbl.gov

[1] So-called disconnected contractions, which are expensive to compute, cancel in isovector observables, making them ideal for verifying lattice QCD.

LATTICE RESULTS

We perform calculations using ten ensembles of lattice QCD gauge fields generated with $\mathcal{O}(a^2)$-improved Symanzik gauge action and tree-level clover-improved Wilson fermion action using 2-HEX stout gauge links [17]. Two light u and d (with $m_u = m_d$) and one heavier strange ($m_s \gg m_{u,d}$, tuned to be close to physical) quark flavors are simulated fully dynamically, while effects of heavier quarks are neglected. In addition to varying the pion mass in the range $149 \ldots 357$ MeV, we include different spatial volumes, time extents of the lattice, and one ensemble with a smaller lattice spacing in order to estimate the size of the corresponding systematic effects; see Tab. I. Nucleon matrix elements are extracted from nucleon 3-point functions that are computed with the standard sequential source method. Nucleon field operators are optimized to overlap as much as possible with the single-nucleon ground state at rest by tuning the spatial width of Gaussian smeared quark sources. This width is kept approximately constant at different pion masses to avoid possible bias due to different smearing. In order to discriminate between the ground and excited-state matrix elements on a Euclidean lattice, we vary the timelike distance Δt between nucleon sources and sinks in the 3-point functions. With increasing Δt, excited states in 3-point functions are suppressed as $\sim e^{-\Delta E \Delta t/2}$ and disappear in the $\Delta t \to \infty$ limit, where ΔE is the (potentially m_π-dependent) energy gap to the closest contributing state. However, using a large source-sink separation is impractical, since statistical noise grows rapidly with Δt. Instead, we combine calculations with three values of $\Delta t \approx 0.9,\ 1.2,\ 1.4$ fm using the summation method [16], which benefits from improved asymptotic behavior [18, 19] and which we find the most reliable and robust method with the presently existing statistics. In a separate publication [20] we report detailed studies and comparisons of different methods, including GPoF [21] and n-state fits.

We present and discuss our results for all the observables in Figs. 1–5 below. To emphasize the importance of controlling excited states, in the same figures we also show the standard plateau method results with fixed Δt (open symbols) for the three lightest m_π used in fits. As this separation is increased, the data points consistently approach our final results, while their error bars increase as expected. As illustrated by the data, the effect of the excited states may be very dramatic, especially for $(r_1^2)^v$, $\kappa^v (r_2^2)^v$ and $\langle x \rangle_{u-d}$.

Our lightest pion mass value $m_\pi = 149(1)$ MeV is only $\approx 10\%$ higher than the physical pion mass in the isospin limit $m_\pi \approx 134.8$ MeV [22]. Since we still have to extrapolate our data in m_π, we select two additional ensembles with the next-lightest pion masses 202(1), 254(1) MeV and the largest spatial volumes to keep model and systematic bias minimal. Table II contains details of fits, results and comparison with experiment. To check the consistency of the low-energy theory, we repeat chiral fits using the full available range of $m_\pi = 149 \ldots 357$ MeV. In general, the results from $m_\pi \lesssim 350$ MeV and $m_\pi \lesssim 250$ MeV fits agree well within error bars, demonstrating good convergence of ChPT.

To explore nucleon electromagnetic structure, we compute matrix elements of the quark-nonsinglet vector current $\langle p' | \big[\bar{u}\gamma_\mu u - \bar{d}\gamma_\mu d\big] | p \rangle$ between polarized proton (uud) states with different momenta p, p'. We extract isovector Dirac and Pauli form factors $F_{1,2}^v(Q^2)$ from these matrix elements, and then the "radii" $(r_{1,2}^2) = -\frac{6}{F_{1,2}} \frac{dF_{1,2}}{dQ^2}\Big|_{Q^2=0}$ using dipole fits $F_{1,2}(Q^2) \sim \frac{F_{1,2}(0)}{(1+Q^2/M_D^2)^2}$ in the range

TABLE I. Lattice QCD ensembles. The strange quark mass m_s is tuned to be close to physical.

a [fm]	$L_s^3 \times L_t$	m_π [MeV]	$m_\pi L_s$	$m_\pi L_t$	# confs	# meas
0.116	$48^3 \times 48$	149(1)	4.20	4.20	646	7752
0.116	$32^3 \times 48$	202(1)	3.80	5.70	457	5484
0.116	$32^3 \times 96$	253(1)	4.78	14.3	202	2424
0.116	$32^3 \times 48$	254(1)	4.78	7.17	420	5040
0.116	$24^3 \times 48$	254(1)	3.58	7.17	419	10056
0.116	$24^3 \times 24$	252(2)	3.57	3.57	1125	6750
0.116	$24^3 \times 48$	303(2)	4.28	8.55	128	768
0.090	$32^3 \times 64$	317(2)	4.64	9.28	103	824
0.116	$24^3 \times 24$	351(2)	4.97	4.97	420	2520
0.116	$24^3 \times 48$	356(2)	5.04	10.1	127	762

TABLE II. ChPT extrapolations to the isospin-limit $m_\pi^{\rm phys} = 134.8$ MeV [22] using data points $149 \le m_\pi \le 254$ MeV. The footnotes describe details of ChPT and fixed parameters in the fits. The right column shows the deviation from experiment, relative to the lattice uncertainty.

X		$X^{\rm lat}$	χ^2/dof	$X^{\rm exp}$		$\frac{X^{\rm lat} - X^{\rm exp}}{\delta X^{\rm lat}}$
$(r_1^2)^v$[fm^2]	[a]	0.577(29)	0.8/2	0.579(3)	[23][g]	−0.07
	[ab]	0.643(29)	4.0/2			+2.21
κ_v	[ac]	3.69(38)	1.3/1	3.706	[24]	−0.04
$\kappa_v (r_2^2)^v$[fm^2]	[ad]	2.46(25)	1.2/2	2.47(7)	[24]	−0.04
$\langle x \rangle_{u-d}$	[e]	0.140(21)	0.9/1	0.155(5)	[25]	−0.71
g_A	[f]	0.97(8)	0.13/1	1.2701(25)	[24]	−3.75

[a] SSE $\mathcal{O}(\epsilon^3)$ [26] with fixed $F_\pi^0 = 86.2$ MeV [27], $\Delta = 293$ MeV [10], $g_A^0 = 1.26$ [4, 28–30], $c_A = 1.5$ [10].
[b] No Δ resonance ($c_A \equiv 0$).
[c] Includes $(N\Delta)_{M1}$ transition with $c_V = -2.5$ GeV^{-1} [31].
[d] Includes higher-order "core" term [32].
[e] BChPT $\mathcal{O}(p^2)$ [33] with fixed $F_\pi^0 = 86.2$ MeV [27], $g_A^0 = 1.26$ [4, 28–30], $M_N^0 = 0.873$ [10], $\Delta a_{20}^v = 0.165$ [34].
[f] SSE $\mathcal{O}(\epsilon^3)$ [28] with fixed $F_\pi^0 = 86.2$ MeV [27], $\Delta = 293$ MeV [10], $c_A = 1.5$ [10], $g_1 = 2.5$ [35].
[g] From r_E^p [23] and $(r_E^2)^n$ [24]. Using Ref. [24] for both $(r_E^2)^{p,n}$ results in $(r_1^2)^v = 0.640(9)$ (higher exp. point in Fig. 1).

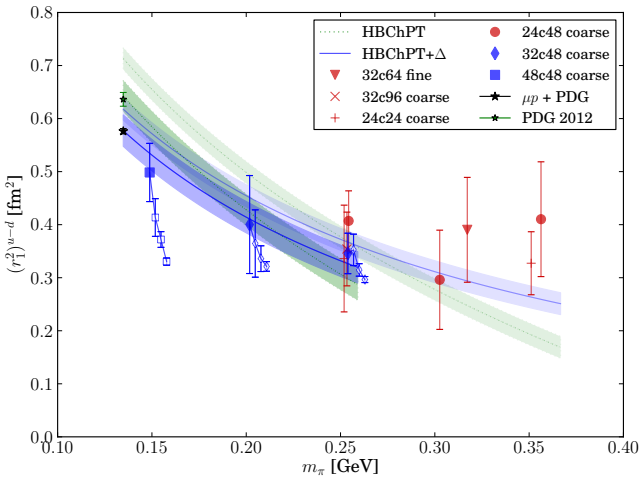

FIG. 1. Isovector Dirac radius $(r_1^2)^v$. Fits to the blue solid square and diamond points are described in Tab. II, and the same fits applied to the full set of solid points are shown for comparison. The two experimental points are from PDG [24] and the μp Lamb shift [23]. The series of open symbols show data before the removal of excited states, with fixed source-sink separation Δt increasing from right to left. Their error bars reflect only statistical errors, which grow with Δt.

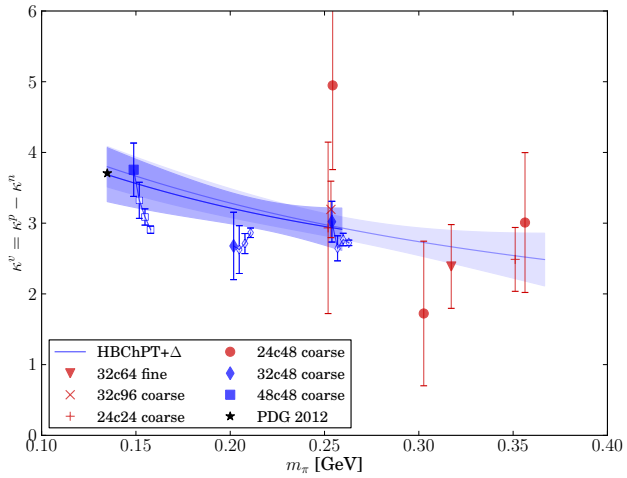

FIG. 2. Isovector anomalous magnetic moment κ^v. See caption of Fig. 1.

$0 \le Q^2 \le 0.5$ GeV^2.

The Dirac radius $(r_1^2)^v$ is shown in Fig. 1. We compare it to the experimental value $(r_1^2)^v = (r_1^2)^p - (r_1^2)^n$, where $(r_1^2)^{p,n} = (r_E^2)^{p,n} - \frac{3\kappa^{p,n}}{2M_{p,n}^2}$, with the error bar dominated by the uncertainty in $(r_E^2)^p$, the proton electric charge radius. We show two experimental values for $(r_1^2)^v$ in Fig. 1, which correspond to two inconsistent values for $(r_E^2)^p$: the PDG value [24] and the recent and controversial result from measurement of the μp Lamb shift [23]. Relative to the lattice uncertainty, the extrapolated value deviates from the μp Lamb shift value by -0.07σ and

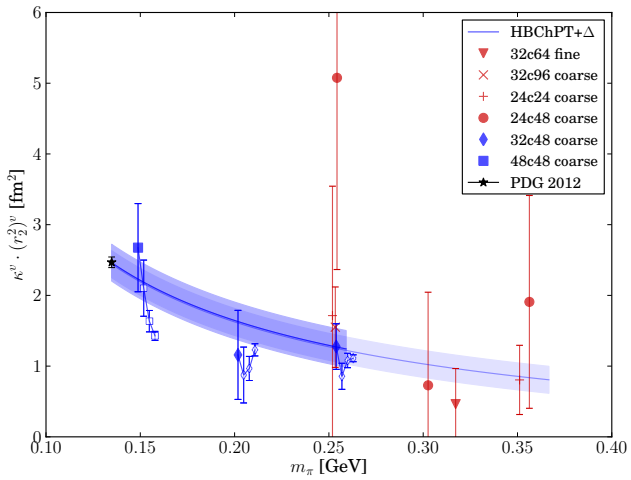

FIG. 3. Isovector Pauli radius $\kappa^v (r_2^2)^v$. See caption of Fig. 1.

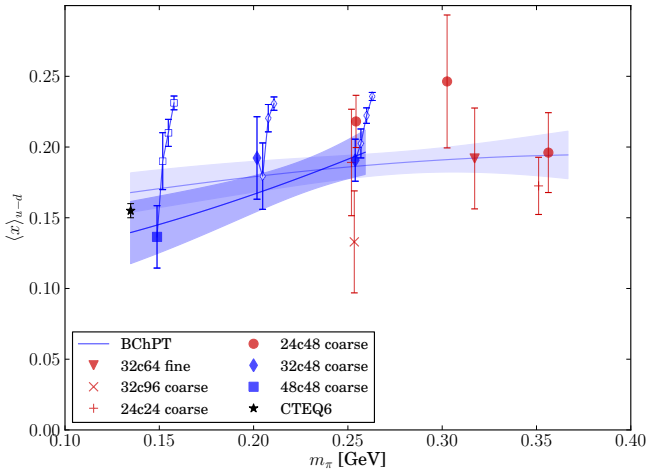

FIG. 4. Isovector quark momentum fraction $\langle x \rangle_{u-d}$. See caption of Fig. 1.

from the PDG value by -2.17σ. In addition, we check the low-energy QCD dynamics by repeating the ChPT fit without the Δ-resonance, shown as the dotted lines in Fig. 1. In this case, we observe somewhat worse fit quality (see Tab. II, line 2), especially when the full m_π range is included in the fit, demonstrating the relevance of the Δ-resonance.

In a similar fashion, we extract the isovector anomalous magnetic moment $\kappa^v = \kappa^p - \kappa^n$ and the Pauli radius $(r_2^2)^v = (\kappa^p (r_2^2)^p - \kappa^n (r_2^2)^n)/(\kappa^p - \kappa^n)$ from the Pauli form factor $F_2(Q^2)$. In this case the results are less precise because the forward values $F_2(0)$ and $\frac{dF_2(0)}{dQ^2}$ are extrapolated using the dipole form $F_2^v(Q^2) \sim \frac{\kappa^v}{(1+Q^2/M_{D2}^2)^2}$. Since the minimal value $Q^2 > 0$ scales roughly as $Q^2_{\rm min} \sim \frac{1}{L_s^2}$, the Q^2 fits are less precise on lattices with smaller spatial volumes. This explains the significant increase of error bars in Figs. 2, 3 going from 32^3 to 24^3 lattices

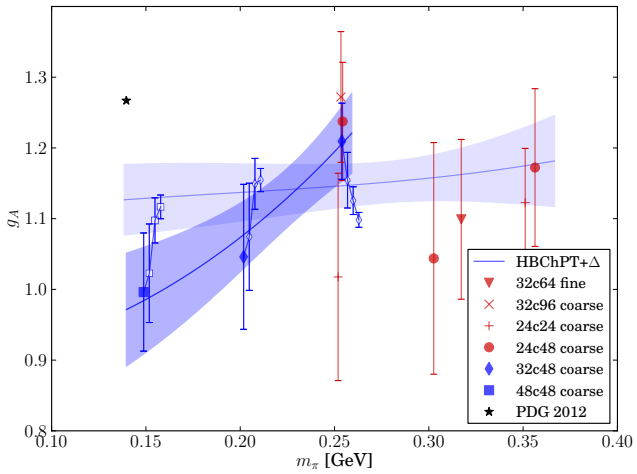

FIG. 5. Axial charge g_A. See caption of Fig. 1.

(e.g., at $m_\pi \approx 250$ MeV), compared to the corresponding error bars of $(r_1^2)^v$ in Fig. 1. However, our results at the lightest pion mass are computed with the largest $V_3 \approx (5.6\text{ fm})^3$ yielding the smallest $Q^2_{\text{min}} \approx 0.05\text{ GeV}^2$ and are the least prone to this problem. For simplicity, we fit and compare to experiment the combination $\kappa^v(r_2^2)^v$, because this quantity is more natural for ChPT than the radius $(r_2^2)^v$ itself. We achieve remarkable agreement both for the anomalous magnetic moment κ^v and the isovector Pauli radius $(r_2^2)^v$.

We compute the isovector quark momentum fraction[2] $\langle x\rangle_{u-d}$ from the forward matrix element of the operator in Eq. 2 and renormalize the lattice value to the standard $\overline{\text{MS}}$(2 GeV) scheme using the *RI'/MOM* method [36]. In Fig. 4 we show ChPT extrapolation curves together with the CTEQ6 phenomenological value [25]. Achieving agreement between the lattice result and phenomenology for $\langle x\rangle_{u-d}$ is one of the most important accomplishments of this paper: previous lattice calculations [12, 35, 37] consistently overestimated the phenomenological value. Our removal of excited state contamination eliminated the discrepancy.

In stark contrast with the observables discussed above, the computed value of the nucleon axial charge g_A strongly disagrees with $g_A^{\text{exp}} = 1.2701(25)$ [24]. There is a notable tendency that g_A^{lat} monotonically decreases with $m_\pi \to m_\pi^{\text{phys}}$ for $m_\pi \lesssim 250$ MeV, increasing the discrepancy with g_A^{exp}. It is remarkable that our results for $m_\pi \gtrsim 250$ MeV agree with the recent calculation [9] that used similar techniques, but decrease dramatically for lighter pion masses. Apparently, there is a source of bias at light pion masses that affects the axial charge significantly more than the other observables discussed above. According to Ref. [13], finite volume effects (FVE) may lead to a 9% bias in g_A at $m_\pi L_s \approx 4.5$ in calculations with domain wall fermions, and as much as $\approx 25\%$ in calculations with $N_f = 2$ flavors of Wilson fermions. However, from our data, it seems very unlikely that FVE can explain the deviation of our near-physical pion mass result from experiment: assuming that the FVE correction scales as $\delta^{\text{FVE}} g_A \sim e^{-m_\pi L}$ analogously to Ref. [13] and using the g_A values from the two lattices with $m_\pi \approx 250$ MeV that differ only in spatial volume ($m_\pi L_s = 3.6$ and 4.8), we obtain an estimate $\delta^{\text{FVE}} g_A = 0.02(8)$ for $m_\pi = 149$ MeV, $L_s = 5.6$ fm, which is much smaller than the observed discrepancy $\delta g_A \approx -0.3$. On the other hand, the data with $m_\pi \lesssim 250$ MeV hint that thermal states [38] may cause a significant bias. For example, pion states are suppressed only by a factor $e^{-m_\pi/T} = e^{-m_\pi L_t}$, and may be natural candidates to make large contributions to matrix elements of the axial current. Although the statistics are not sufficient to draw a solid conclusion, at given pion mass the central values of g_A in Fig. 5 monotonically rise with $m_\pi L_t = 3.6...14.3$ (see Tab. I), supporting this hypothesis. This effect appears to weaken in the vicinity of $m_\pi L_t \sim 7.2$.

DISCUSSION

The crucial departure of this work from previous calculations lies in the careful control of excited-state contaminations in nucleon matrix elements on lattices almost all the way down to the physical pion mass. We have shown that, although this is multiplicatively more computationally expensive (in this case, $\times 3$), such control is essential for extracting correct results from lattice QCD at the physical pion mass and reproducing experimental values of nucleon structure observables.

We have carried out calculations with a range of pion masses and consistently applied the robust summation technique to remove excited states. In addition, we have performed some limited checks of finite volume and discretization effects. For the first time, we have achieved agreement with experiment for all the reported quantities except the axial charge g_A. This agreement is strong evidence that this combination of methods is sufficient to correctly estimate and remove systematic errors in most nucleon structure calculations. Our results suggest that the disagreement in the axial charge value is due to the insufficient temporal extent of the lattice, which is equivalent to having non-zero temperature in the system.

Additional statistics are necessary to improve the precision of the reported results, since the errors are still much larger than in experiments. Nevertheless, the remarkable precision of the computed isovector Dirac ra-

[2] $\langle x\rangle_{u-d} = \langle x\rangle_u - \langle x\rangle_d$ is understood as the momentum fraction carried by quarks *and* antiquarks, i.e. $\langle x\rangle_q = \int_0^1 dx\, x\,\left(f_q(x) + f_{\bar{q}}(x)\right)$, where $f_{q(\bar{q})}$ is a parton distribution function (PDF).

dius $(r_1^2)^v$ is already comparable to the discrepancy between the two contradictory experimental values, and future improvements may be able to contribute to a resolution of this discrepancy.

More lattice spacings and further volumes and temporal extents at pion masses below 200 MeV are required to put stronger bounds on other sources of systematic uncertainty. With appropriately increased statistics, our control over excited-state contamination could be cross-checked by further varying the nucleon source-sink separation and by comparing against other excited state removal techniques.

It is encouraging that Lattice QCD, for many important benchmark quantities, now is in good agreement with experimental results.

ACKNOWLEDGEMENTS

We thank Zoltan Fodor for useful discussions and the Budapest-Marseille-Wuppertal collaboration for making some of their configurations available to us. This research used resources of the Argonne Leadership Computing Facility at Argonne National Laboratory, which is supported by the Office of Science of the U.S. Department of Energy under contract #DE–AC02–06CH11357, and resources at Forschungszentrum Jülich. During this research JRG, SK, JWN, AVP and SNS were supported in part by the U.S. Department of Energy Office of Nuclear Physics under grant #DE–FG02–94ER40818, ME was supported in part by DOE grant #DE–FG02–96ER40965, SNS was supported by Office of Nuclear Physics in the US Department of Energy's Office of Science under Contract #DE–AC02–05CH11231, and SK was supported in part by Deutsche Forschungsgemeinschaft through grant SFB–TRR 55.

[1] J. Ellis, K. A. Olive, and P. Sandick, New J.Phys., **11**, 105015 (2009), arXiv:0905.0107 [hep-ph].
[2] T. Bhattacharya, V. Cirigliano, S. D. Cohen, A. Filipuzzi, M. Gonzalez-Alonso, *et al.*, (2011), arXiv:1110.6448 [hep-ph].
[3] J. Green, J. Negele, A. Pochinsky, S. Syritsyn, M. Engelhardt, *et al.*, (2012), arXiv:1206.4527 [hep-lat].
[4] R. Edwards *et al.* (LHPC Collaboration), Phys.Rev.Lett., **96**, 052001 (2006), arXiv:hep-lat/0510062 [hep-lat].
[5] P. Hägler *et al.* (LHPC), Phys. Rev., **D77**, 094502 (2008), arXiv:0705.4295 [hep-lat].
[6] T. Yamazaki *et al.*, Phys. Rev., **D79**, 114505 (2009), arXiv:0904.2039 [hep-lat].
[7] C. Alexandrou, M. Brinet, J. Carbonell, M. Constantinou, P. Harraud, *et al.*, Phys.Rev., **D83**, 094502 (2011), arXiv:1102.2208 [hep-lat].
[8] S. Collins, M. Göckeler, P. Hägler, R. Horsley, Y. Nakamura, *et al.*, Phys.Rev., **D84**, 074507 (2011), arXiv:1106.3580 [hep-lat].
[9] S. Capitani, M. Della Morte, G. von Hippel, B. Jäger, A. Jüttner, *et al.*, (2012), arXiv:1205.0180 [hep-lat].
[10] S. Syritsyn, J. Bratt, M. Lin, H. Meyer, J. Negele, *et al.*, Phys.Rev., **D81**, 034507 (2010), arXiv:0907.4194 [hep-lat].
[11] C. Alexandrou, J. Carbonell, M. Constantinou, P. Harraud, P. Guichon, *et al.*, Phys.Rev., **D83**, 114513 (2011), arXiv:1104.1600 [hep-lat].
[12] G. S. Bali, S. Collins, M. Deka, B. Glaessle, M. Göckeler, *et al.*, (2012), arXiv:1207.1110 [hep-lat].
[13] T. Yamazaki *et al.* (RBC+UKQCD Collaboration), Phys.Rev.Lett., **100**, 171602 (2008), arXiv:0801.4016 [hep-lat].
[14] C. Alexandrou *et al.* (ETM Collaboration), Phys.Rev., **D83**, 045010 (2011), arXiv:1012.0857 [hep-lat].
[15] J. Green, S. Krieg, J. Negele, A. Pochinsky, and S. Syritsyn, PoS, **LATTICE2011**, 157 (2011), arXiv:1111.0255 [hep-lat].
[16] N. Mathur, S. Dong, K. Liu, L. Mankiewicz, and N. Mukhopadhyay, Phys.Rev., **D62**, 114504 (2000), arXiv:hep-ph/9912289 [hep-ph].
[17] S. Dürr, Z. Fodor, C. Hoelbling, S. Katz, S. Krieg, *et al.*, JHEP, **1108**, 148 (2011), arXiv:1011.2711 [hep-lat].
[18] S. Capitani, B. Knippschild, M. Della Morte, and H. Wittig, PoS, **LATTICE2010**, 147 (2010), arXiv:1011.1358 [hep-lat].
[19] J. Bulava, M. Donnellan, and R. Sommer (ALPHA Collaboration), PoS, **LATTICE2010**, 303 (2010), arXiv:1011.4393 [hep-lat].
[20] LHP collaboration, "Nucleon form factors with (2+1) Wilson fermions," (2012), in preparation.
[21] C. Aubin and K. Orginos, AIP Conf.Proc., **1374**, 621 (2011), arXiv:1010.0202 [hep-lat].
[22] G. Colangelo, S. Dürr, A. Jüttner, L. Lellouch, H. Leutwyler, *et al.*, Eur.Phys.J., **C71**, 1695 (2011), arXiv:1011.4408 [hep-lat].
[23] R. Pohl *et al.*, Nature, **466**, 213 (2010).
[24] J. Beringer *et al.* (Particle Data Group), Phys.Rev., **D86**, 010001 (2012).
[25] Durham Database Group, Durham University (UK),.
[26] V. Bernard, H. W. Fearing, T. R. Hemmert, and U. G. Meissner, Nucl. Phys., **A635**, 121 (1998), arXiv:hep-ph/9801297.
[27] G. Colangelo and S. Dürr, Eur.Phys.J., **C33**, 543 (2004), arXiv:hep-lat/0311023 [hep-lat].
[28] T. R. Hemmert, M. Procura, and W. Weise, Phys. Rev., **D68**, 075009 (2003), arXiv:hep-lat/0303002.
[29] A. A. Khan *et al.*, Phys. Rev., **D74**, 094508 (2006), arXiv:hep-lat/0603028.
[30] M. Procura, B. Musch, T. Hemmert, and W. Weise, Phys.Rev., **D75**, 014503 (2007), arXiv:hep-lat/0610105 [hep-lat].
[31] T. R. Hemmert and W. Weise, Eur.Phys.J., **A15**, 487 (2002), arXiv:hep-lat/0204005 [hep-lat].
[32] M. Göckeler *et al.* (QCDSF), Phys. Rev., **D71**, 034508 (2005), arXiv:hep-lat/0303019.
[33] M. Dorati, T. A. Gail, and T. R. Hemmert, Nucl. Phys., **A798**, 96 (2008), arXiv:nucl-th/0703073.
[34] R. G. Edwards *et al.*, PoS, **LAT2006**, 121 (2006), arXiv:hep-lat/0610007.

[35] J. Bratt *et al.* (LHPC Collaboration), Phys.Rev., **D82**, 094502 (2010), arXiv:1001.3620 [hep-lat].

[36] G. Martinelli, C. Pittori, C. T. Sachrajda, M. Testa, and A. Vladikas, Nucl. Phys., **B445**, 81 (1995), arXiv:hep-lat/9411010.

[37] Y. Aoki, T. Blum, H.-W. Lin, S. Ohta, S. Sasaki, *et al.*, Phys.Rev., **D82**, 014501 (2010), arXiv:1003.3387 [hep-lat].

[38] S. R. Beane *et al.*, Phys. Rev., **D79**, 114502 (2009), arXiv:0903.2990 [hep-lat].